CHAPTER 3

MODELING OF COSMIC RAY DETECTOR OPERATION

CALIBRATION OF THE AUGER WATER CHERENKOV DETECTOR

M. Anguiano[1], A. Fernandez[1], G. K. Garipov[2], B. A. Khrenov[2], O. Martinez[1], H. Salazar[1], L. Villasenor[3], and A. Zepeda[4]

The Auger Water Cherenkov Detector (WCD) prototype (area 10 m^2) was constructed at the campus of Puebla University at an elevation of 2.2 km above sea level. Differential and integral spectra of cosmic ray energy depositions in the WCD were measured. The results of these measurements are discussed. The problem of the WCD "self-calibration" (by rates of muon events) is considered. The characteristic change in slopes of the differential spectrum at the transition from single muon signals to EAS signals is also discussed. The distribution of EAS signals observed at the level of Puebla University is compared with the sea level data. The results we obtained are discussed from the standpoint of WCD applications in the Auger array.

1. Introduction. The Water Cherenkov Detector (WCD) installed in the Pierre Auger Observatory array for studying high energy cosmic rays is the basic Extensive Air Shower (EAS) particle detector. The WCD is a circular tank of diameter 3.6 m filled with water up to a height of 1.2 m. Three PhotoMultiplier Tubes (PMTs) of diameter 20 cm each are completely submerged in water. These tubes are used to observe the Cherenkov light generated in water by fast EAS charged particles. One can find a detailed description of this WCD in [1]. Since there are thousands of WCDs allocated at the observatory (each of them operating for a long time), the monitoring of all their parameters makes a serious problem. In the large EAS arrays installed at Haverah Park, Yakutsk, and Akeno, the monitoring of particle detectors was performed by an analysis of the detector signal response to the commands from a registration center as well as by an analysis of the events selected by a detector "local" trigger. The EAS selecting system operates in the following two stages: at the first stage, each detector selects the signal that is not associated with the EAS and at the second stage, the true EAS events are selected by comparison of signals from several detectors. The local trigger rate was used as an estimator of the detector operation in the arrays of Haverah Park and Yakutsk. Modern technology of detector controllers allows us to use more detailed information on the detector response to the local trigger: for example, the spectrum of energy depositions in the WCD and the signal width distribution can be analyzed. In principle, this information given for each PMT of the detector makes it possible to perform the complete calibration of detector signals in units standard for all array detectors. To use this "self-calibration" method, information on the performance of the WCD triggered by local events should be collected and analyzed.

With this aim in view, the Puebla University full-size prototype of the WCD has been tested. The results of measurements of the WCD energy deposition spectrum and the signal width distribution are presented here; preliminary results were published at the Utah conference [2, 3]. In this paper, the experimental results are compared with the expected spectrum caused by cosmic rays at an elevation of Puebla University, where the average atmospheric depth is 800 g/cm^2.

2. Experimental setup and control experiments. In the prototype setup, two types of PM tubes were tested. Hamamatsu R5912 tubes were used at the first stage of operation and EMI-3954 tubes at the second stage. The setup electronics allows us to measure and to summarize signals from each tube. A full description of the electronic equipment was published in [4]. The WCD measures the energy deposition of fast charged

[1] Facultad de Ciencias Fisico Matematicas, Universidad Autonoma de Puebla, Apdo. Postal 1364, Puebla, México, e-mail: afernand@fcfm.buap.mx; omartin@fcfm.buap.mx; hsalazar@fcfm.buap.mx

[2] Skobeltsyn Institute of Nuclear Physics, Moscow State University, Moscow, 119899, Russian Federation, e-mail: garipov@eas.npi.msu.ru; khrenov@eas.npi.msu.ru

[3] Instituto de Física y Matemáticas, U. Michoacan, A. Postal 2-82, 58040, Morelia Michoacan, Mexico, e-mail: villasen@zeus.ccu.umich.mx

[4] Depto de Física, Cinvestav-IPN, 07000, Mexico D. F., Mexico, e-mail: zepeda@fis.cinvestav.mx

particles traversing the water of the detector. The light signal can be measured by the PMTs in units of the number n of photoelectrons (p.e.) generated at the tube cathodes or in units of the charge $C = enK$ collected at the tube anodes, where e is the electron charge and K is the PMT gain. The anode peak amplitude is a possible measure of energy deposition if the signal shape is constant in time. This is not the case when the EAS pulses are registered (that is why the charge C is more preferable as an energy deposition estimator).

The signal of 1 p.e. was measured in the control experiment. Each PMT was placed into a sealed box, where it was illuminated by pulses from a Light Emission Diode (LED). The signals from a tube were synchronized with an LED generator. The amplitudes of the generator pulses were selected so small that only 1/10 of the LED pulses could produce signals in the tube. It was shown that the 1p.e. resolution in EMI tubes is better than in Hamamatsu tubes. In the EMI tubes, the peaks corresponding to 2 and 3 p.e. were detected, while the Hamamatsu tubes resolve only a 1 p.e. peak. The width of charge distribution of signals with n p.e. was found to be approximately (with an accuracy up to 10 %) equal to $1/\sqrt{n}$, as might be expected if the first dynode gain fluctuation is much less than a statistical fluctuation of the p.e. number. It was also proved that the p.e. number determined by a statistical method (by measuring the root mean square of signal fluctuations) coincides with the number determined as the ratio of a signal charge to the 1 p.e. charge. For each tube, the gain as a function of the voltage was checked in measurements of the anode charge for signals given in number of p.e. ($n = 1$–20). Those calibration functions for each tube were used for measurements of the tube signals in number of p.e.

At the first stage of setup operation, the anode charge spectrum of each tube was measured and the voltage on tubes was adjusted to make all the three spectra identical.

The reference signal in the Auger detectors is the signal from the vertical muon (called the "Vertical Equivalent Muon (VEM) signal"). This signal is measured with the aid of the "telescope" of two scintillation pads placed beneath and above the water tank. The rate of VEM events is 0.3 s^{-1} for two scintillation pads of area 800 cm^2. The absolute muon intensity was measured with the aid of the telescope of two scintillation pads of area 225 cm^2 each. The pairs of pads operating in coincidence were separated by a distance of 100 cm. To separate vertical electrons from muons, the following two measurements were done: for the first measurement, the lower pad was covered by a 10 cm iron filter and for the second one, there was no filter. Without a filter, the rate of two-fold coincidences was 0.110 s^{-1}; with an iron filter, the rate was 0.085 s^{-1}. The rates of local showers with and without a filter were also measured as two-fold coincidences of the same pads placed in a horizontal plane and separated by a distance of 60 cm. The local showers had rates 0.025 s^{-1} with no filter and 0.015 s^{-1} with the filter. Extracting the rates of the local showers from the telescope rate, we found that the total intensity of vertical charge particles at the campus of Puebla University was equal to $I_{\rm ch} = 0.017$ cm^{-2} s^{-1} sr^{-1} and the intensity of vertical muons was equal to $I_\mu = 0.014$ cm^{-2} s^{-1} sr^{-1}.

The charge distribution summarized over the three tube anodes is represented in Figure 1 (Curve a) for signals selected by the "telescope". The average VEM signal is equal to $n = 57 \pm 3$ in number of p.e. The deviation σ of the VEM signal charge distribution is equal to $\sigma = 0.2$ VEM $= 12$ p.e. (presumably, it is a sum of statistical fluctuations $\sigma_s \simeq 7.5$ p.e. in number of p.e. and of energy deposition fluctuations $\sigma_e \simeq 9$ p.e.).

The average VEM signal we obtained depends on various factors: the tank water quality, the reflectivity of the inner tank walls (in fact, on the reflectivity of the liner that contains water), the optical properties of the PM tube windows, and the optical couplings between a tube window and a liner window. Monitoring of the VEM signal is a way of monitoring the WCD operation.

The temporal profile of a WCD signal was measured with the aid of a digital oscilloscope [4]. For the comparison with the previously measured [5] temporal characteristics of WCD signals, the oscilloscope profiles were integrated and the signal "rise time" was obtained as in [5]. The rise time T_1 between signal levels of 10 % and 50 % of the integrated value and the time T_9 between levels of 10 % – 90 % were determined. The average rise times of VEM signals were found to be equal to $T_1 = 16.5 \pm 0.5$ ns and $T_9 = 75 \pm 5$ ns. In the first approximation, the width distributions are Gaussian with $\sigma_T/T = 0.2$. The VEM signal duration is mainly determined by the time of light collection in the tank and is long in comparison with the 1 p.e. signal duration ($T_9 = 12$ ns). The observed VEM signal width distribution corresponds to the fluctuation in light arrival at the tube cathodes.

When the arrival of EAS particles is considered, the VEM signal width should be treated as the "instrumental width" caused by the intrinsic detector properties. The width of signals from the EAS could be much larger than the "instrumental width".

3. Experimental results. The differential spectra of the WCD energy depositions C selected with a threshold of 0.2 VEM is represented in Figure 1 (Curve b) in the range of $C = 0.2$ – 3 VEM. Measurements were done with the aid of the electronics different from [4]: signal charges integrated in time 100 ns were measured

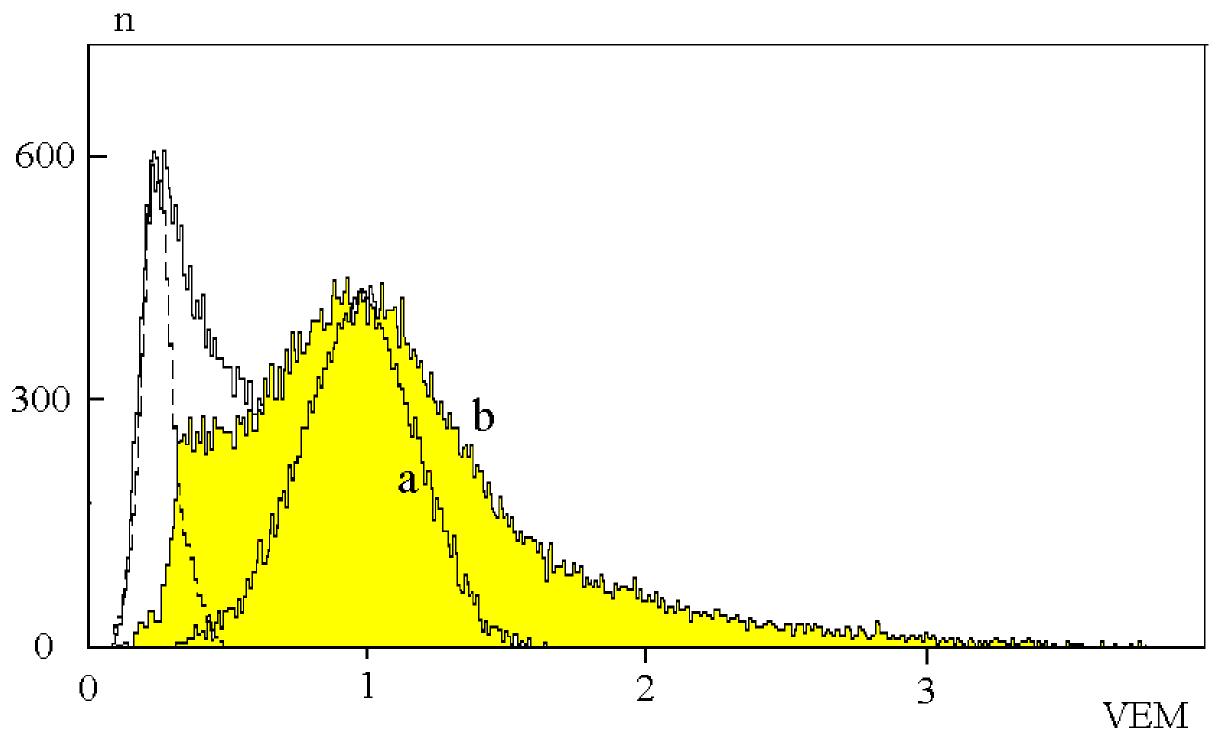

Fig. 1. The differential WCD energy deposition C-spectrum. The C-interval is equal to 0.005 VEM.
Curve a: for muons selected by the scintillation telescope (vertical muons). Number of muons 48000.
Curve b: for all signals above a threshold of 0.2 VEM. Number of events 84300.
The solid line — the experimental spectrum, the dashed line — the spectrum of noise, the shadowed area — the true experimental spectrum minus noise)

by an ADC (Amplitude Digital Converter) in a CAMAC acquisition system. With this electronics, the signal rate in KHz is easily measured, in contrast to the equipment proposed in [4] for the registration of temporal profiles. In Figure 1, the values of experimental charges are expressed in VEM units and the instrumental pedestal of C-values is taken into account.

The noise at a threshold of 0.2 VEM was essential. It was measured separately, with the PM tube voltage off (the dashed curve in Figure 1). The WCD rate for the threshold 0.2 VEM after the extraction of noise is 2.16 kHz. The "true" charge distribution is depicted by the shadowed area. The maxima of all event distributions practically coincides with the maximum of the distribution of vertical muons. Simulation of ionization energy losses by muons traversing the detector showed that the plateau in the left-hand part of the shadowed area is due to the yield of "clipping" muons. The number of clipping muons is small in comparison with the bulk of all muons traversing the detector. It is an important feature of a large detector (in a detector of smaller area 2 m^2, clipping muons form a large part of the spectrum [4]) that allows us to define the reference VEM signal without the scintillation telescope. The spectrum of all WCD signals is wider ($\sigma = 0.3$) than for the vertical muons due to the variation in geometry of the muon passages through the water of the tank. The smallest signals are from "clipping" muons passing through only a part of the available water. Large signals are from the muons that have the path $L = h/\cos\vartheta$, where h is the vertical path and ϑ is the muon zenith angle. The largest "geometrical" signals are for the diagonal passages of $L = 3.8$ m ($C = 3.2$ VEM).

For the signals with $C > 2$ VEM, other phenomena become also important. The differential (a) and integral (b) C-distributions in the range of $1-100$ VEM are presented in Figure 2.

For the signals of about 2 VEM, the C-distribution changes from "geometrical" shapes to a power law with the differential exponent 4.33. For the signals of about 5 VEM, the power law exponent changes from 4.33 to a more flat distribution. The range of the signals with $C = 2-5$ is presumably a region of the secondary showers produced in water by cosmic ray muons and hadrons (see [6]).

The next region ($C \gg 5$) is a region of the EAS signals. The EAS energy deposition is a sum of energy

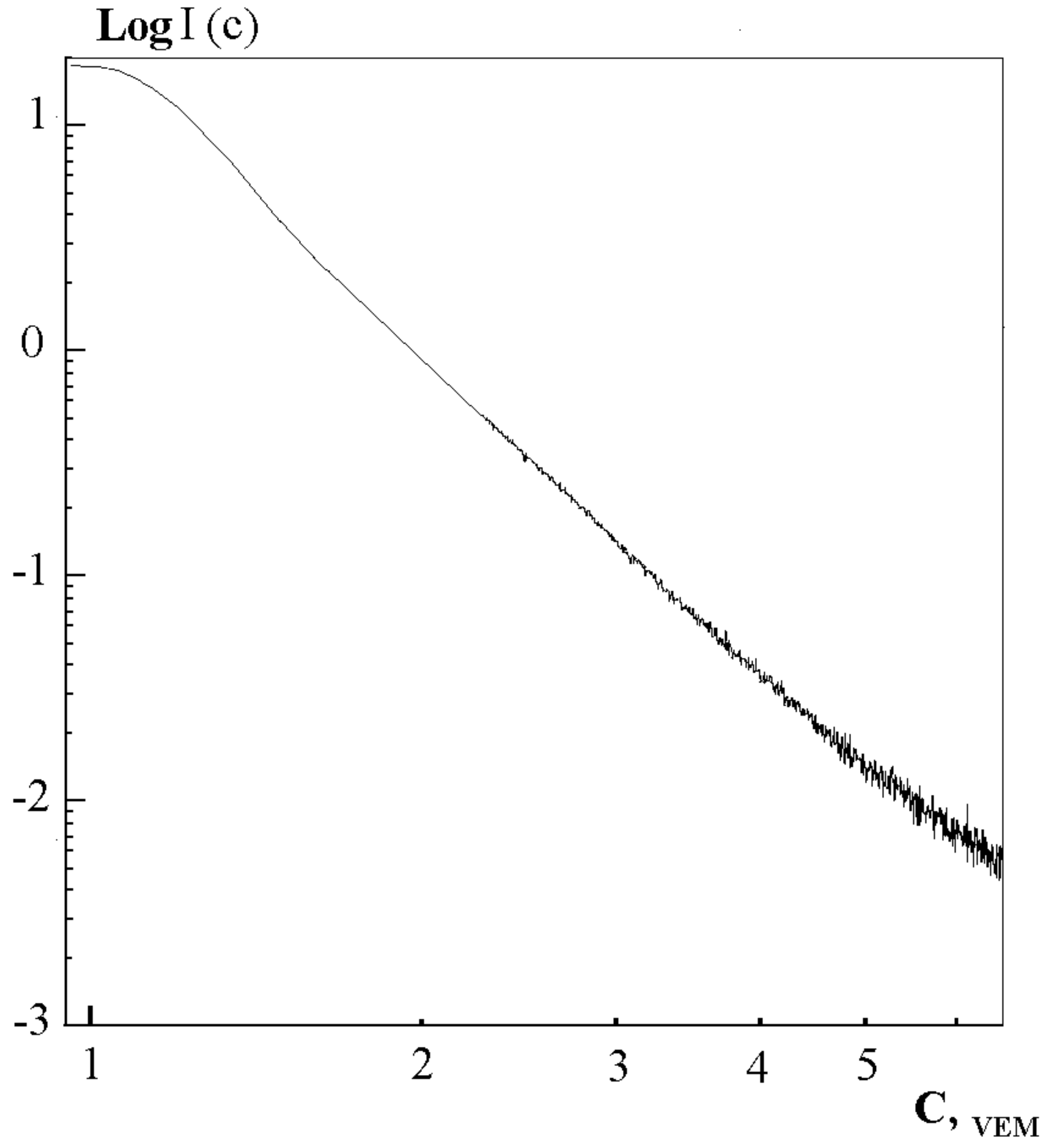

Fig. 2 a. The experimental WCD energy deposition spectrum: differential spectrum. The C-interval is 0.005 VEM. In the Y-axis, the rate in Hz per the differential C-interval is presented

depositions from all EAS components: the electromagnetic component (electrons plus photons converted to electrons in water), muons and hadrons (producing the secondary showers in water). A shape of the energy deposition spectrum is determined by the expected EAS energy deposition "density" spectrum (an analog of the EAS density spectrum measured by thin scintillation detectors or by other detectors sensitive to the flux of EAS charge particles). The relation between the EAS density spectrum and the cosmic ray primary energy spectrum $I(E)$ is well known [7]. In a simple case, when the particle Lateral Distribution Function $f(R)$ (LDF) is independent of the primary energy E, the energy deposition density is determined by the primary cosmic ray energy spectrum (let it be presented by the power law $I(E) = E^{-(\gamma+1)}$) and by the "density" energy dependence $C(E,R) = aE^b f(R)$. In this case, the EAS energy deposition spectrum is equal to

$$I(C)\,dC = aKC^{-(\gamma/b+1)}\,dC \tag{1}$$

where K is the integral over the core distance:

$$K = \int 2\pi R f^{\gamma/b}(R)\,dR \tag{2}$$

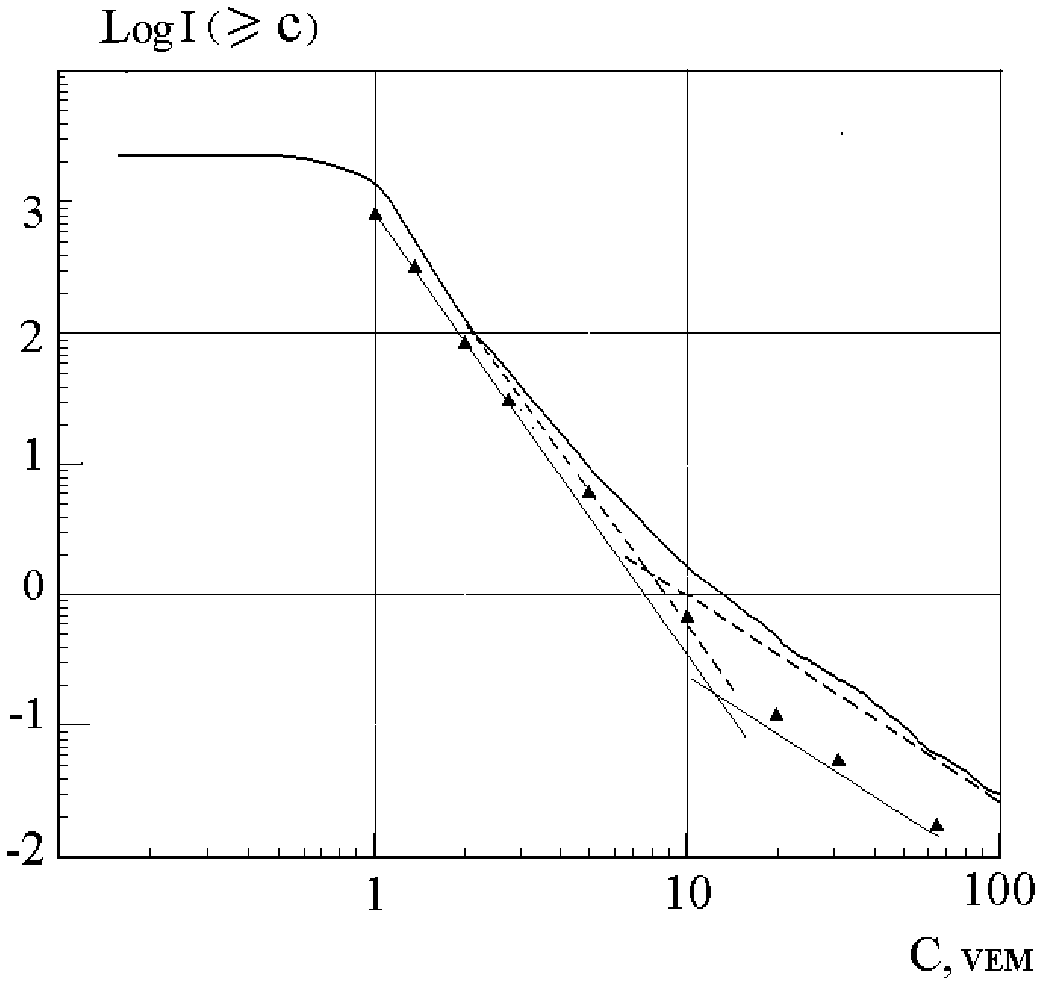

Fig. 2 b. The experimental WCD energy deposition spectrum: integral spectrum. The event rate is given in Hz. The dashed lines represent the two slopes with exponents 3.33 and 1.5 discussed in the text. The thin lines represent the spectrum slopes at sea level expected from the data obtained. The triangles indicate the experimental data [6] at sea level normalized at $C = 1$ VEM to the data expected from the experiment performed

Extracting single muon events from all events (the spectrum with the slope 4.33), we found the following differential EAS "energy deposition density" spectrum (in the WCD of area $S = 10$ m^2):

$$I(C) = 51C^{-2.50\pm0.03}\ \mathrm{s}^{-1} \tag{3}$$

where C is given in VEM.

Summarizing the WCD experimental data at the level of Puebla University, we can approximate the experimental data on the differential spectrum as a sum of the three components:

— the Gaussian distribution of single-muon passages:

$$G_1 = 1.76\times 10^3/\sqrt{2\pi}\,\sigma \exp\left[(C-1)^2/2\sigma^2\right]\ \mathrm{s}^{-1}, \quad \sigma = 0.35, \quad C < 2\ \mathrm{VEM} \tag{4}$$

(the yield of small signals from clipping muons is ignored);

— the power law of energy depositions from single-muon interactions:

$$J_2 = 4.3\times 10^3/C^{4.33}\ \mathrm{s}^{-1}, \quad C \geqslant 1.5\ \mathrm{VEM} \tag{5}$$

— the power law of the EAS “density” spectrum:

$$J_3 = 51/C^{2.50}\ \mathrm{s}^{-1}, \quad C \geqslant 2\ \mathrm{VEM} \tag{6}$$

The integral rates of events in a standard WCD of area $S = 10$ m^2 at the air pressure $X = 800$ g/cm^2 and temperature 25° C are shown in Table 1.

Table 1: The rate of the WCD events with energy depositions more than C in VEM

C, VEM	0.2	1	2	5	10	30
Rate, Hz	2160	1220	140	9.1	1.7	0.22

The atmospheric depth dependence of those components of rates is expected to be exponential but with different absorption path lengths λ: for single muons $\lambda_\mu = 630$ g/cm^2 and for EAS $\lambda_{\mathrm{eas}} = 140$–150 g/cm^2 ($\lambda_{\mathrm{eas}}$ for the WCD energy depositions was measured in [8]). Using (4) – (6) for the experimental data at the level of Puebla University ($X_{\mathrm{P}} = 800$ g/cm^2), we can predict the energy deposition spectrum in the WCD ($S = 10$ m^2) at other levels X (g/cm^2) in the atmosphere:

$$I_{\mathrm{wcd}}(C, X) = G_1 \exp\bigl[-(X - X_{\mathrm{P}})/\lambda_\mu\bigr] + J_2 \exp\bigl[-(X - X_{\mathrm{P}})/\lambda_\mu\bigr] + J_3 \exp\bigl[-(X - X_{\mathrm{P}})/\lambda_{\mathrm{eas}}\bigr] \tag{7}$$

In Figure 2 b, the expected integral WCD energy deposition spectrum at sea level (the dashed line) is compared with the spectrum at the level of Puebla University. The experimental data [6] at sea level are in agreement with the data of our experiments. At sea level, the intersection range of two slopes — 3.33 and 1.5 — is slightly shifted to higher depositions due to the absorption of the EAS.

It should be noted that the transition range from single muon events to EAS events is rather wide: the experimental integral spectrum exponent is changing gradually with C (it is equal to 2.45 at $C = 5$–10 VEM, to 1.85 at $C = 10$–30 VEM, and to 1.6 at $C = 30$–100 VEM). The experimental data could be used in approximate form (4) – (7) as reference data for WCDs at various atmospheric depths (pressures). The difference in correlation of the rate of two components (muon and EAS signals) with atmospheric pressure should be taken into account. The above-presented absorption path lengths correspond to the following atmospheric pressure coefficients: for muons it is 2 % per cm Hg and for EAS it is 9.3 % per cm Hg. We also found that there is an instrumental rate variation with the day/night temperature: the rate increases with temperature by 1 % per degree of Celsius.

4. WCD signals in the EAS range. For the Auger array, the EAS signals are of special interest. The yield of various core distances R to a given energy deposition C is a key function for the estimation of an expected temporal shape of the EAS signals. For core distances $R > 50$ m, the energy deposition LDF and the dependence of the EAS signal width on the core distance are known experimentally (the data obtained at Haverah Park, sea level, [1, 5, 9]). At sea level, the expected spectrum of EAS energy depositions, the yield of various core distances R, and the primary energy E can be calculated for a given deposition by formulas (1) – (2). In the first approximation, we will assume that at the level of Puebla University the WCD energy deposition LDF is the same as at sea level, but the absolute energy deposition “density” is $\exp\bigl[(1020 - 800)/\Lambda\bigr]$ times higher than that for the same primary energy E (Λ is the absorption length for the EAS energy deposition in the WCD: $\Lambda = \lambda_{\mathrm{eas}}\gamma/b = 210$ g/cm^2). A difficulty in the above calculations is that the LDF is not experimentally approved for $R < 50$ m; we avoid this difficulty by comparison of the rates of expected and calculated EAS events with a given energy deposition.

We started with the Haverah Park LDF approximated in [9] as

$$H(E, R, \vartheta) = cE^b / R^{3.49 - 1.29 \sec\vartheta + 0.15 \log(E/0.1) + R/4000} \tag{8}$$

Here H is the WCD energy deposition density VEM/m^2 and the primary energy E is in EeV. The energy dependence of absolute values of H was not specified in [9]. We set the coefficient c and the exponent b to be $c = 1.23 \times 10^7$ and $b = 1.4$ in order for the absolute density at the core distance 600 m in the range $E = 0.1$–10 EeV to be equal to the values assumed in the experiments at Haverah Park. In this approximation, the density H at $R = 600$ m is in proportion to the energy E as was proved in [10].

The exponent for all particle primary cosmic ray energy spectra is taken equal to $\gamma = 1.75$ before the knee ($E \leqslant 3$ PeV) and $\gamma = 2.1$ after the knee; the integral primary particle intensity at the energy threshold $E = 1$ PeV is equal to 0.006 h^{-1} m^{-2} sr^{-1}.

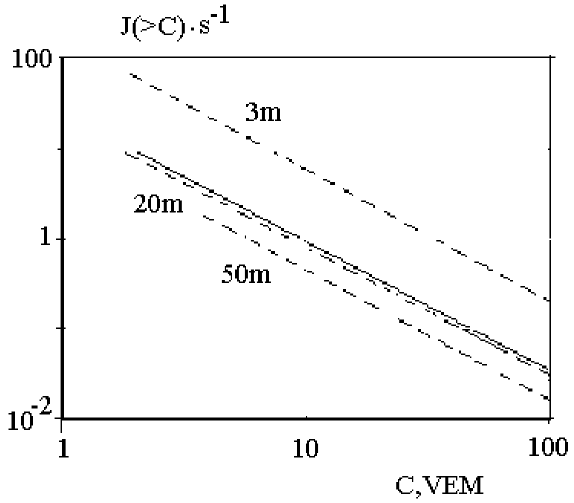

Fig. 3. Comparison of the expected EAS energy deposition integral spectra with the experimental WCD rates. The solid curve — the experimental rates. The dashed curves — the expected rates for Haverah Park LDF with various limit distances R_c indicated on the curves

The calculated integral EAS energy deposition spectrum at the level of Puebla University is shown in Figure 3 together with the experimental data approximated as (3). The yield of core distances R to the energy deposition $C = 30$ VEM, as expected from the Haverah Park LDF, is given in Figure 4 (the solid line). In those calculations, approximation formula (8) was extrapolated from small distances $R < 50$ m to some limit R_c and the expected intensity of the energy deposition spectrum for various R_c was compared with the experimental integral intensity 0.22 s^{-1} for $C_{\mathrm{thr}} = 30$ VEM. It was found that the expected spectrum intensity agrees with the experiment for $R_c \simeq 25$ m (i.e., at distances $R < 50$ m the energy deposition LDF should be much flatter than the extrapolation by formula (8)).

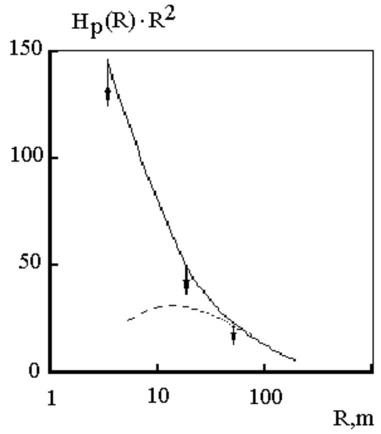

Fig. 4. Calculated yield of core distances R to the given WCD energy deposition $C = 30$ VEM. The solid line — the Haverah Park LDF, the arrows indicate $R_c = 3$ m, $R_c = 20$ m, and $R_c = 50$ m. The dashed line — the Yakutsk LDF normalized to the Haverah Park LDF at $R = 100$ m

It should be noted that the experimental LDF of energy depositions in thin scintillation detectors is really flatter than (8), though at distances $R > 100$ m it is similar to the water Cherenkov detector LDF. We calculated the density spectrum in the scintillation detector, using the above approach. The following formula for the scintillation detector LDF was used (this formula was introduced to approximate the experimental data [10] obtained in Yakutsk):

$$Y(E,R) = 2.2 \times 10^5 E^{1.2}/R(1+R/70)^{2.2+0.17\log E} \tag{9}$$

Here $Y(E,R)$ is the charge particle density in VEM/m^{-2} (for the scintillation detector).

As in (8), approximation formula (9) includes the energy dependence factor $E^{1.2}$, which is needed to fit the density at $R = 600$ m in proportion to the primary energy. The absolute values of density at $R = 600$ m in the WCD and scintillation detectors are different: $Y/H = 1.7$ due to a different amount of matter in the detectors. The density spectrum in the scintillation detector calculated with the use of LDF (9) is in agreement with the experiments at sea level (see, for example, [6]). For LDF (9), the yield of distances R to a given energy deposition in the scintillation detector is represented in Figure 4 (the dashed line). The effective core distances for a given energy deposition are of about 20 m, i.e., in agreement with our estimate for the WCD LDF. This allows us to suppose that the shape of the WCD LDF at distances $R < 100$ m is similar to the shape of the scintillation detector LDF (this assumption has to be checked in direct experiments).

For the WCD LDF extrapolated by (9) from distances $R > 50$ m to small core distances, the effective primary energies responsible for the depositions at the level $C = 1$ and $C = 10$ (in VEM/m^2) are: $E = 0.18$ PeV and $E = 1.3$ PeV. This means that for a WCD of area 10 m^2 the energy deposition spectrum at $C < 280$ VEM is related to the primary energy spectrum before the knee (primary energies less than 3 PeV). In this case, the exponent of the integral WCD energy deposition spectrum is expected to be equal to the ratio $1.75/b'$, where b' is the exponent in the dependence of $C(E, R_{\text{eff}} \simeq 25\ \text{m}) \approx E^{b'}$ (R_{eff} presents distances R effective for a given signal C). For the WCD energy deposition approximated as (8), the exponent b' is equal to 1.14 and the experimental exponent 1.50 ± 0.03 of the energy deposition spectrum is in agreement with the expected value $1.75/1.14 = 1.53$ (the exponent of the scintillation detector density spectrum is almost the same: $1.75/1.16 = 1.5$).

The WCD experimental data on large energy depositions in a domain of the EAS depositions can be used as a test of linearity of the WCD response to the EAS signals. The slope of the spectrum obtained at Puebla in the range of energy depositions up to 100 VEM (Figure 2) agrees with the expected EAS spectrum.

5. The Auger array trigger. The events with large core distances $R > 1$ km to be selected by the Auger final trigger (the coincidence of signals in several WCD separated by the distance $L = 1.5$ km) are extremely rare among the events with a given energy deposition. The expected ratio of events with core distances $\geqslant R$ to all EAS events is represented in Figure 5 (in this calculation, the Haverah Park LDF was used). For $R = 1.5$ km, it is about 0.001.

To select the EAS with a minimum energy threshold, the signal threshold in each WCD must be at the lowest level $C_{\text{thr}} = 0.3$ VEM. The number of WCDs triggered in a selected event must be high enough to put a limit for random coincidences. For example, to get the random rate less than 1 Hz, the five-fold coincidences (with time resolution 5 μs) of adjacent WCDs are needed.

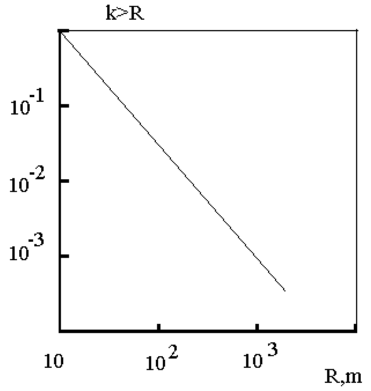

Fig. 5. The expected ratio of EAS events with core distances $\geqslant R$ to all EAS events with a fixed WCD energy deposition

This "ideal" EAS trigger is difficult for realization. The Auger communication and data acquisition systems put a limit of 20 Hz for the rate of each WCD. A straightforward way to reach the WCD rate at a level of 20 Hz is to use $C_{\text{thr}} = 4$ VEM. With this C_{thr}, the EAS energy threshold will be much higher than the "ideal" one.

An additional cut-off of the useless signals could be achieved if the pulses longer than the single muon pulses are selected for the array triggering. The Haverah Park experimental dependence of the EAS signal rise time T_1 (defined above) on the core distance R and zenith angle ϑ (this dependence is discussed in [1]) can be approximated in the following form:

$$T_1(R, \vartheta) = 8 \cos^{2.4} \vartheta \, (1 + R/50)^{1.2} \text{ ns}, \quad R \text{ in m} \tag{10}$$

Our experimental data show the existence of WCD signals whose width is much larger than the instrumental one. The correlation plot of the rise times T_1/T_9 observed in one run of the WCD operation is shown in Figure 6 (for $C_{\rm thr} = 3$ VEM). There is a region of well-correlated points of wide signals, beyond the region of the instrumental width presented by the intensive rate of signals (the black region in Figure 6).

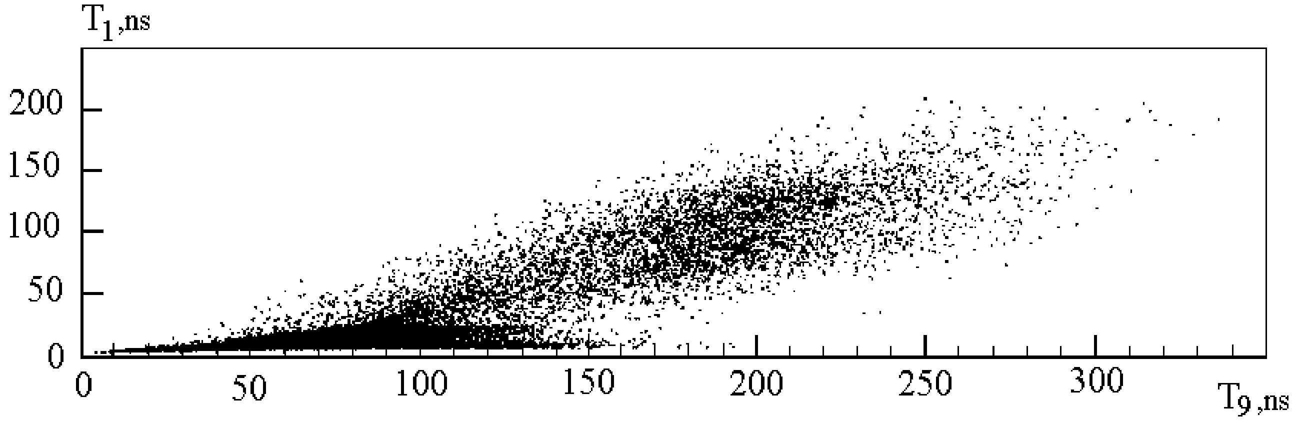

Fig. 6. The experimental plot of observed correlation between the rise time T_1 and the rise time T_9 in the WCD run with the threshold $C_{\rm thr} = 3$ VEM

Using relation (10), we calculated the expected EAS rise time distribution as a transform of core distance distribution (2). The instrumental width distribution was taken into account in a Gaussian form ($\langle T_1 \rangle = 16.5$ ns, $\sigma_T = 3$ ns). The calculated rate of EAS signals for various $C_{\rm thr}$ turned out to be in agreement with our experimental data: for $C_{\rm thr} = 1$ VEM, the events with rise time $T_1 \geqslant 25$ ns are recorded with a rate of $\simeq 10$ Hz ($\simeq 0.5\%$ of all events), for $C_{\rm thr} = 3$ VEM this percentage is $\simeq 2\%$, and for $C_{\rm thr} = 10$ VEM it is $\simeq 15\%$. Presumably, the signals with $T_1 \geqslant 25$ ns are signals from the EAS with core distances greater than some threshold $R_{\rm thr}$ dependent on T_1 as (10).

Table 2:

ϑ, degree	10	30	40	50	60
$R_{\rm thr}$, m	85	125	170	265	470

A way of selecting the width threshold should be a compromise between the needed cut-off for useless single muon events and a not-rigid threshold for core distances recorded in the Auger array. For an energy deposition threshold of 1 VEM and a rise time threshold T_1 of 25 ns, a rate of 10 Hz is less than the limit 20 Hz put by the Auger data acquisition system. To make a final decision about this kind of EAS selection criteria, we should check how rigid this criterion is with respect to the selection of large distances at various EAS zenith angles. The core distance thresholds predicted by formula (10) for various values of the zenith angle ϑ and for the rise time threshold $T_1 = 25$ ns are represented in Table 2.

In our example, the threshold $T_1 = 25$ ns allows us to select the EAS with the core distance $R' = R_{\rm thr}/\cos\vartheta$ in the observation plane in such a way that R' is much less than the WCD separation length $L = 1500$ m at zenith angles $\vartheta \leqslant 50°$, i.e., practically for all zenith angles available for measurements by the Auger array.

The above discussion allows us to suggest the following criterion for the local Auger trigger: the energy deposition $C \geqslant 1$ VEM and, at the same time, the signal rise time $T_1 \geqslant 25$ ns. The expected trigger rate is about 10 Hz. It should be noted that the signals that satisfy this criterion will be initiated mostly by the EAS electromagnetic component. A 1 VEM signal roughly corresponds to a signal from 3–10 electrons — the number large enough to produce a spread signal (but small enough to be a subject of fluctuations). The fluctuation factor is enlarged because of the presence of muon signals. In some signals, one muon may appear first; after it, a much larger number of electrons should appear (to compensate the fast large signal of muon). In general, this trigger will be biased to a muon-poor EAS (at the array energy threshold). In order to equalize the amplitudes of muons and electrons, the muon signal amplitude has to be cut off at the level of electron amplitude (as is in thin scintillator plates). This could be done after an additional analysis of temporal profiles of the WCD signal. The WCD electronics allows us to perform this analysis.

6. Conclusion. The data obtained with the aid of the above WCD prototype show that the detector construction allows us to receive data on particle energy depositions in water for a wide range of depositions and to control the detector performance on-line, using the rate of energy depositions from muons.

The calibration procedure (the definition of a VEM signal) could be performed without a scintillation telescope selecting vertical muons. The signal where the maximum of energy deposition distribution in a WCD of area $S = 10$ m^2 is observed can be considered as a good reference VEM signal.

The rate of signals at larger than VEM thresholds ($C = 2, 5, 10$) could be used for testing the precise performance of the detector. Corrections should be applied due to an elevation of the detector and the atmospheric pressure.

The selection of EAS events in the Auger array by the local WCD trigger could be performed with a not-rigid criterion for the energy deposition $C \geqslant 1$ VEM if, at the same time, the selection by the signal width $T_1 \geqslant 25$ ns is introduced and, in the analysis of the WCD signal temporal profile, the muon signals are made equivalent to the electron ones.

The comparatively short instrumental rise time of WCD signals ($T_1 = 16$ ns) allows us to use these detectors for the study of temporal profiles of EAS pulses at core distances greater than 500 m. We plan to use WCDs in the array at a mountain level for the study of an early stage of EAS development (before and near the cascade maximum) at the primary energies 10^{16}–10^{18} eV.

REFERENCES

1. The Pierre Auger Project Design Report, November, 1996.
2. A. Fernandez et al., *ICRC-26*, Salt Lake City, **2**: 377, 1999.
3. A. Fernandez et al., *ICRC-26*, Salt Lake City, **2**: 381, 1999.
4. V. Alarcon et al., *NIM, A*, **420**: 39, 1999.
5. A.A. Watson and J.G. Wilson, *J. Phys. A, Math., Nucl. Gen.*, **7**: 1199, 1974.
6. H.R. Allan et al., *ICRC-9*, London, **1**: 678, 1965.
7. K. Greisen, in: *Progress in Cosmic Ray Physics*, **3**: 7, 1956.
8. J.D. Hollows, H.W. Hunter, and A.N. Suri, *J. Phys. A* (*Gen. Phys.*), **2**: 591, 1969.
9. C. Prike et al., *Astroparticle Physics*, **263**: 270, 1997.
10. A.J. Bower et al., *J. Phys. G, Nucl. Part. Phys.*, **9**: L53, 1983.
11. N.N. Efimov et al., "Astrophysical aspects of the Most Energetic Cosmic Rays", *World Scientific*, p. 20, 1991.